ACS NANO

www.acsnano.org

ARTICLE

Understanding Chemistry of Two-Dimensional Transition Metal Carbides and Carbonitrides (MXenes) with Gas Analysis

Shuohan Huang and Vadym N. Mochalin*

Cite This: *ACS Nano* 2020, 14, 10251−10257

Read Online

ACCESS | Metrics & More | Article Recommendations | Supporting Information

ABSTRACT: **MXenes, a large family of two-dimensional materials that are intensely investigated for a broad range of applications, are unstable in water, spontaneously forming TiO_2. Several hypotheses have been proposed recently to explain the transformations of MXenes in aqueous environments based on characterization of solid products and measurements of solution pH. However, no studies of the gaseous products of these reactions have been reported. In this work, we demonstrate the use of Raman spectroscopy and gas chromatography techniques to study the gaseous reaction products of Ti_2C, Ti_3C_2, Ti_3CN, and Nb_2C MXenes in aqueous environments. Based on the analysis of gases, the reactivities of MXenes with different monolayer thickness and chemical composition have been analyzed. We demonstrate the analysis of gases produced during MXene transformations as a powerful technique that can be used for better understanding of their nontrivial chemistry.**

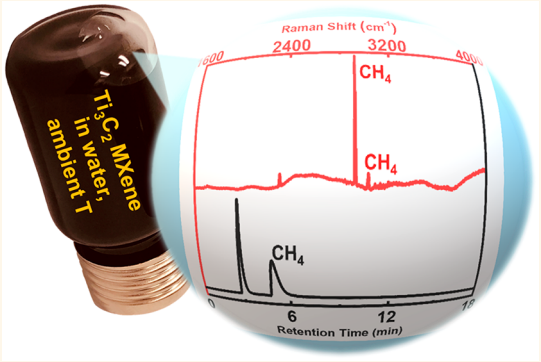

KEYWORDS: *MXene chemistry, gas analysis, reactivity of 2D materials, gas chromatography, Raman spectroscopy*

Two-dimensional (2D) materials have raised significant interest due to their many outstanding properties. MXenes are a large family of two-dimensional early transition metal carbides/nitrides discovered in 2011.[1,2] They are produced by selective extraction of group A element atoms (typically Al) from bulk precursor MAX phases using fluorine-containing etchants. MXenes have a general formula $M_{n+1}X_nT_x$, where n = 1−4, M represents an early transition metal, X is carbon or nitrogen, and T stands for surface terminations (−OH, −F, and −O−) whose fraction in the formula is usually unknown (x).[3] Because of their 2D structure and outstanding combination of properties,[2,4] MXenes have demonstrated promise in various applications, such as optoelectronic devices,[5] lasers,[6] sensors,[7−9] THz wave transmission and communication technology,[10,11] *etc.* Although the interest in using MXenes for a broad range of applications is quickly growing, their basic chemical properties remain largely unexplored. This is particularly worrisome because MXenes, especially in their most commonly used aqueous colloidal state, are known to be unstable, spontaneously transforming into the corresponding M element oxides over time, resulting in structure degradation and loss of properties.[12−14] Not surprisingly, attempts have been reported to protect MXenes against oxidation, particularly in aqueous solutions.[15−17] However, in most of these reports, only indirect evidence (such as electrical conductivity or electrochemical performance) was used to demonstrate the suppression of MXene degradation. Although important from a practical standpoint, the indirect evidence of prolonged MXene stability may not reflect the real degree of chemical transformations in the system. Therefore, the question as to the extent of MXene degradation, even in the situations when it was reportedly suppressed, still remains open. Besides practical importance, direct studies of MXene transformations may shed more light onto currently poorly understood chemistry of 2D transition metal carbides and nitrides. Whereas the fate of transition metal atoms (most typically titanium) in the processes of MXene degradation is more or less clear (they end up in the corresponding transition metal oxides, *e.g.*, titanium oxide), much less is known about the fate of carbon and nitrogen atoms of MXenes. Some reports mention that the oxidative degradation of Ti_3C_2 MXene in aqueous solutions yields

Received: April 29, 2020
Accepted: July 9, 2020
Published: July 9, 2020

https://dx.doi.org/10.1021/acsnano.0c03602
ACS Nano 2020, 14, 10251−10257

Table 1. Description of Experiments Conducted in This Study

name	brief description	purpose
experiment 1	10 mL glass headspace vial fully filled with MXene solution and sealed, kept at 70 °C upside down with a plastic needle inserted through septum as outlet with the other end of the needle submerged in water	collect enough volume of gas for GC measurements
experiment 2	20 mL closed glass vial filled with 10 mL solution kept at 70 °C in sand bath	1. pH measurements over time 2. separate supernatant from solid after complete degradation of Ti_3CN for ATR FTIR measurements 3. separate solid phases from MXene solutions after their complete degradation for Raman measurements
experiment 3	10 mL headspace vial filled with 6 mL solution and sealed, then kept upside down in an oven at 70, 80, and 90 °C, correspondingly	Raman measurements of gas phase over the time of reaction

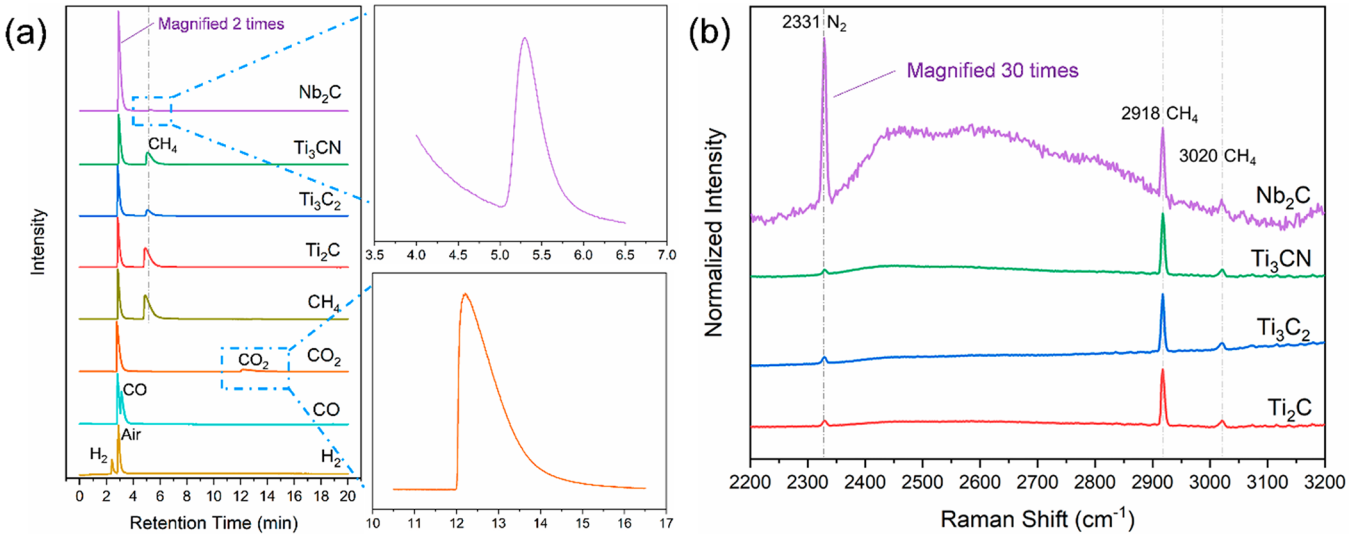

Figure 1. (a) GC analysis of gaseous products of Ti_2C, Ti_3C_2, Ti_3CN, and Nb_2C MXene transformations in water and standard H_2, CO, CO_2, and CH_4 gases. The insets on the right show enlarged areas of CH_4 peak produced in Nb_2C degradation and CO_2 peak of reference CO_2 gas. (b) Raman spectra of gas bubbles collected and analyzed in sealed vials in the course of Ti_2C, Ti_3C_2, Ti_3CN, and Nb_2C MXene transformations in water.

titanium dioxide and CO_2,[18] whereas other authors believe that the final products of MXene degradation are TiO_2 and carbon.[12,13,17,19,20] To our best knowledge, no reports on the degradation products of nitrogen-containing MXenes have been published so far.

As an example of complex chemistry of MXenes, we have recently shown that in addition to oxidation, MXenes directly react with water in ambient conditions.[21] This experimental observation of MXene reactivity toward water in ambient conditions differs from chemistry of their bulk counterparts—transition metal carbides. The interactions of bulk carbides with water and aqueous acid or base solutions have received mixed representation in textbooks and papers. Although reports and common inorganic chemistry textbooks mention that titanium carbide is resistant to decomposition in water as well as aqueous acid and base solutions,[22−24] Avgustinik *et al.*[25] reported long ago the reaction between group IV metal carbides and water yielding hydrocarbons and hydroxides. Their results also showed that the extent of the attack by water is limited by 5−30 surface atomic layers of the carbide, which for a bulk material was properly deemed to be insignificant. However, such an attack will have dramatic consequences in the case of 2D forms of these carbides, where the entire thickness of the monolayer is just several atomic layers. Thus, traditional knowledge of chemistry of bulk carbides can be misleading if transferred directly to carbide-based MXenes.

Clearly, studying MXene reactivity is important for synthesis, storage, device fabrication, as well as almost any of their applications. Water colloids are most commonly used to synthesize, process, and store MXenes and are used in device fabrication. Hence, chemical reactivity of MXenes toward water is of great importance and should be studied further. It is logical to speculate that carbon and nitrogen in the course of these transformations will finally form gaseous species, probably CH_4, CO, CO_2, N_2, *etc.*[21] However, no experimental confirmation of these products has been obtained whatsoever.

In this work, we demonstrate gas analysis as a powerful technique to gain further insights into the chemical reactivity of MXenes. Gases produced during chemical transformations of Ti_2C, Ti_3C_2, Ti_3CN, and Nb_2C MXenes in aqueous colloidal solutions (UV−vis spectra and photographs of these solutions are shown in Figure S1) have been collected and analyzed *via* gas chromatography (GC) and Raman spectroscopy. The degradation rates of the MXenes in water were further investigated depending on their monolayer thickness within the same chemical composition, as well as depending on chemical composition of the materials within the same monolayer thickness.

https://dx.doi.org/10.1021/acsnano.0c03602
ACS Nano 2020, 14, 10251−10257

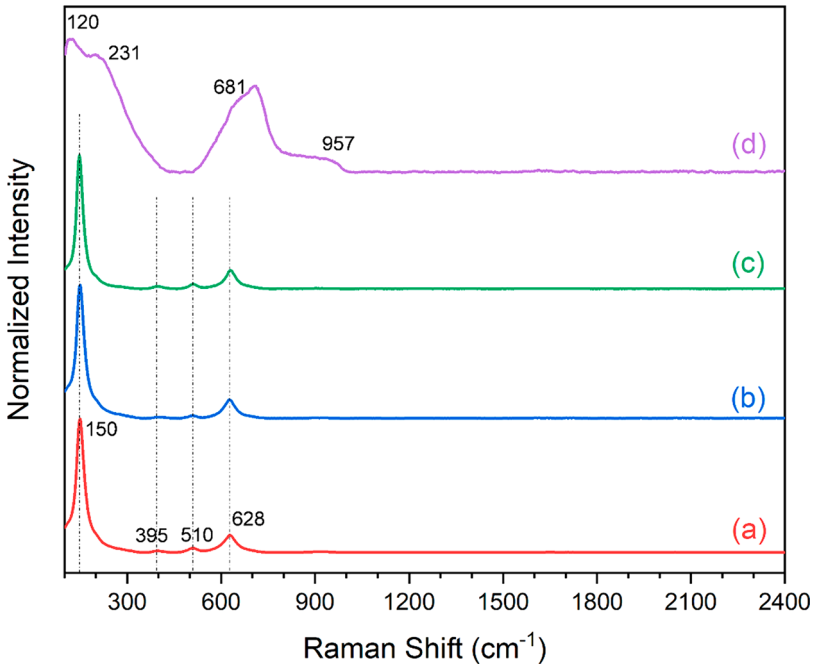

Figure 2. Raman spectra of final solid transformation products of (a) Ti_2C, (b) Ti_3C_2, (c) Ti_3CN, and (d) Nb_2C MXenes in aqueous solutions. Dashed vertical lines mark peak positions of TiO_2 anatase.

RESULTS AND DISCUSSION

Experiments of three types, referred hereafter as experiment 1, 2, and 3 (Table 1; further details are provided in Methods section and Figure S2 in the Supporting Information), were conducted to collect and characterize the transformation products of different MXenes in water. Figure 1a shows chromatograms of the corresponding gas phases collected from experiment 1 with different MXenes, as well as pure H_2, CO, CO_2, and CH_4 gases used as references. Comparison of the retention times allows unambiguous identification of CH_4 as the main gaseous product of the transformations of all four studied MXenes in water (retention time of CH_4 reference in the conditions of our GC experiment is ~5 min; see Supporting Information for gas analysis and material characterization details). This result indicates that carbon in all studied carbide and carbonitride MXene structures ends up forming CH_4 during their transformations in water. Because our GC instrument equipped with a thermal conductivity detector is not particularly sensitive to CO_2 (Figure 1a), we further investigated evolved gas composition using other techniques.

Raman spectra of the gas-phase bubbles produced and collected in sealed glass vials from experiment 1 are shown in Figure 1b. The peak at 2331 cm^{-1} represents the symmetric stretching mode of N_2, which probably originates from the small amount of air dissolved in DI water,[26] whereas the peaks at 2918 and 3020 cm^{-1} correspond to symmetric and asymmetric C−H stretching modes in methane, respectively.[27] Surrounding series of regularly spaced smaller peaks within the 2850−3200 cm^{-1} range represent rotational Raman spectrum of CH_4, as confirmed by the bond length calculation provided in Supporting Information (Figure S3). Thus, Raman spectroscopy provides further strong support to GC observations of methane evolution during the transformations of carbide and carbonitride MXenes in water. In contrast to previously published hypotheses,[18,21] no traces of CO and CO_2 were observed in our experiments either in GC or in Raman, although these gaseous products would be expected in an oxidative degradation of our MXenes.

An alternative hypothesis regarding the fate of carbide carbon during MXene degradation expressed in literature is that it remains in the form of "carbon".[12,13,17,19,20] To test this hypothesis and answer the question whether there is any solid carbon left, we have analyzed solid products of complete MXene degradation from experiment 2 using Raman spectroscopy. Obviously, the M elements in the final solid products are anticipated to form the corresponding metal oxides in all our experiments. Accordingly, Raman spectra of solid transformation products of Ti_2C, Ti_3C_2, and Ti_3CN (Figure 2) show a strong peak at 150 cm^{-1} along with three other peaks at 395, 510, and 628 cm^{-1}, respectively, all of which can be assigned to the anatase form of TiO_2.[19,21] The Raman spectrum of the solid transformation product of Nb_2C shows peaks at 120, 231, 681, and 957 cm^{-1}, representative of Nb_2O_5.[19,28] No peaks have been detected in the range of the Raman shift typical for carbon (1200−1700 cm^{-1}), thus ruling out the hypothesis of solid carbon present in the transformation products of the MXenes. Furthermore, energy-dispersive X-ray spectroscopy (EDS) also shows no traces of carbon or nitrogen in the solid degradation products of different MXenes (Figure S4). Thus, we conclude that titanium carbide MXenes in an aqueous environment ultimately transform into TiO_2 and CH_4, whereas Nb_2C MXene transforms into Nb_2O_5 and CH_4, respectively. These final products are most likely formed in multistage reactions, and detailed mechanisms of their formation still remain unknown.

Another interesting MXene with respect to its chemistry is carbonitride Ti_3CN, especially because chemical transformations of carbonitride MXenes have never been studied previously. Similar to carbon, nitrogen in the MXene structure is expected to form gaseous products. Based on the high strength of the triple bond in N_2, *a priori* there is a high chance that nitrogen atoms from the MXene structure will form N_2

https://dx.doi.org/10.1021/acsnano.0c03602
ACS Nano 2020, 14, 10251−10257

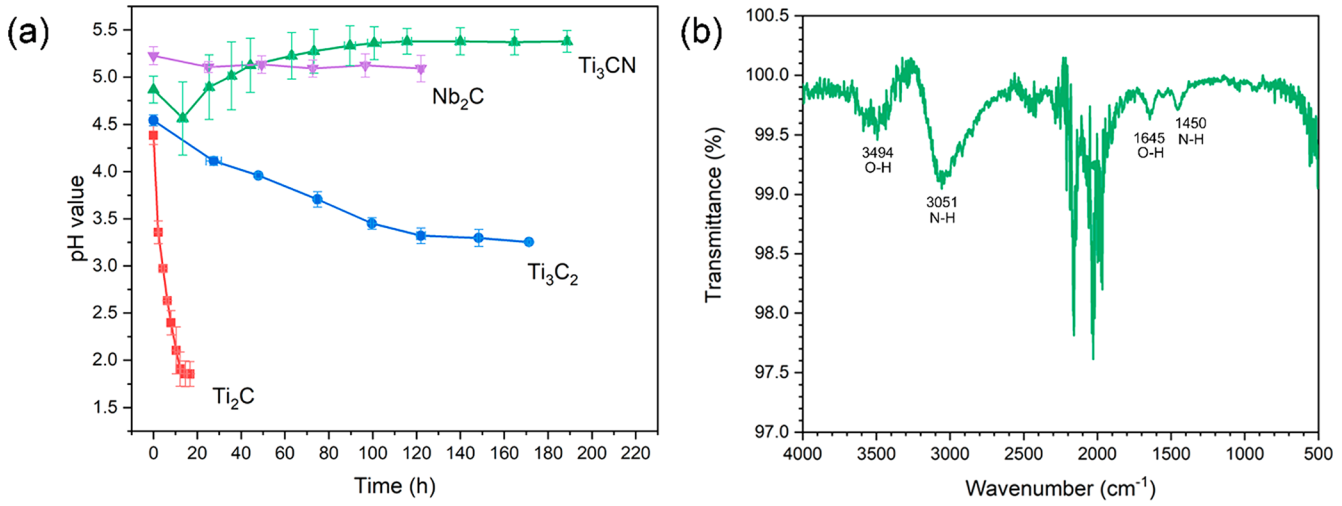

Figure 3. (a) Averaged pH values of Ti_2C, Ti_3C_2, Ti_3CN, and Nb_2C MXene aqueous colloidal solutions kept at 70 °C over time. Error bars indicate standard deviations in time and pH values. (b) ATR FTIR spectrum of liquid supernatant from a fully degraded Ti_3CN solution.

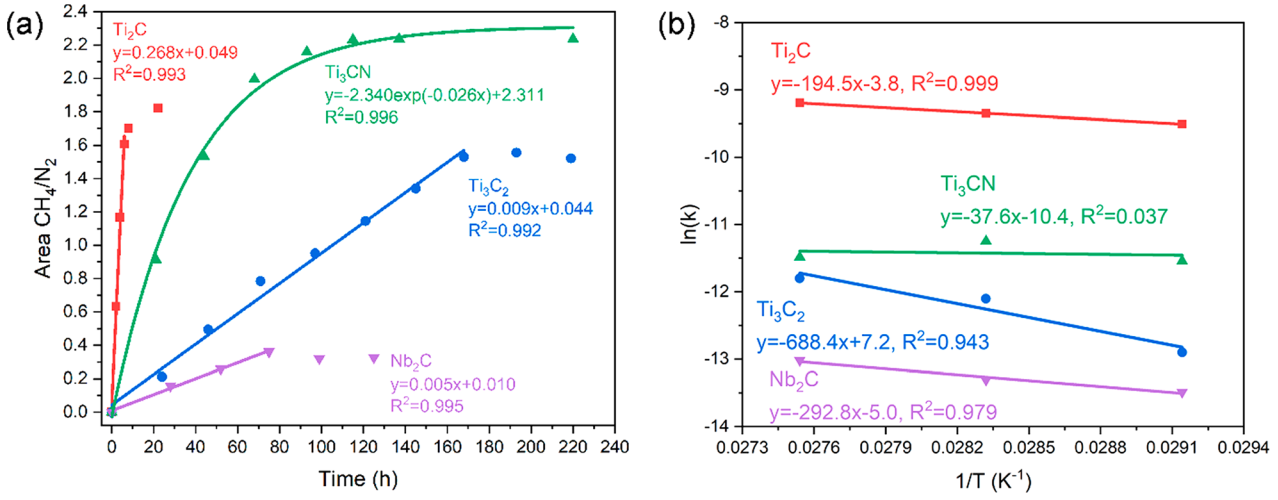

Figure 4. (a) Transformation kinetics of Ti_2C, Ti_3C_2, Ti_3CN, and Nb_2C MXenes in aqueous solutions at 70 °C. Solid lines represent fits to the corresponding color-coded equations indicated in the graph. (b) Arrhenius plots for transformations of Ti_2C, Ti_3C_2, Ti_3CN, and Nb_2C MXenes in water.

gas. However, apart from CH_4, no accumulation of N_2 (besides N_2 from air) nor other gases were detected in the reactions of Ti_3CN with water, neither by GC nor by Raman (Figure 1). Another plausible possibility is the formation of ammonia (NH_3), which further chemically interacts with water, forming NH_4OH. Formation of ammonium hydroxide in the solution must result in the corresponding increase of pH. Thus, an experiment of type 2 was conducted, and pH values of the Ti_3CN aqueous solution were recorded over time during its transformation. The solution was kept in a 70 °C sand bath to accelerate the reactions. For comparison, pH values of Ti_2C, Ti_3C_2, and Nb_2C MXene aqueous colloids were also monitored in same conditions. These pH-monitoring experiments were repeated three times for each MXene, and all collected data are summarized in Figure S5 (Supporting Information). The average pH values shown in Figure 3a initially drop with time over the first ~20 h in Ti_2C, Ti_3C_2, and Ti_3CN solutions, perhaps due to release of the intercalated acidic species (HF or HCl) when MXene structure degrades.[29] The rate of the drop in pH correlates with the MXene degradation rate (compare curves for Ti_2C and Ti_3C_2 in Figure 3a). There is no significant change of pH during the degradation of Nb_2C, perhaps indicating its lower reactivity (also manifested by a lower rate of methane production; see Figure 4a) or low concentration of a Nb_2C colloidal solution. However, as the reaction progressed beyond 20 h, the pH trend of Ti_3CN solution turned from decrease to growth (Figure 3a), in striking difference to other carbide MXene solutions. Therefore, the pH trends support the hypothesis of ammonia formation during Ti_3CN degradation in water. In the presence of anions, ammonium will form the corresponding ammonium salts, which can be discovered using spectroscopic techniques. Indeed, bending (1450 cm^{-1}) and stretching (3051 cm^{-1}) modes[30] of N−H in NH_4^+ were observed in addition to H−O−H bending (1645 cm^{-1}) and O−H stretching (3494 cm^{-1}) vibrations of water[31] in the attenuated total reflection (ATR) Fourier transform infrared (FTIR) spectrum of liquid supernatant collected from Ti_3CN solution after complete MXene degradation (Figure 3b). These results confirm formation of NH_3 (or NH_4^+) during the transformation of Ti_3CN in water. Moreover, the Raman spectrum shows only TiO_2 in the water-rinsed solid degradation products of Ti_3CN

https://dx.doi.org/10.1021/acsnano.0c03602
ACS Nano 2020, 14, 10251−10257

(Figure 2), no solid carbon remains after the degradation. Thus, the combination of results from gas, liquid, and solid products analysis leads us to conclude that the transformation of the titanium carbonitride MXene in water produces TiO_2, CH_4, and NH_3.

One of the unique advantages provided by MXenes is that they allow the effects of material composition to be disentangled from the monolayer thickness effects on various properties (chemical and others) of 2D materials, thus offering a rare opportunity for systematic fundamental studies of these effects in their most pure form.[21,32] To illustrate the effects of the monolayer thickness and chemical composition of a MXene monolayer on the reactivity of the material, we studied kinetics of transformations of different MXenes in water using Raman spectroscopy of gaseous decomposition products, comparing the rates of evolution of their common degradation product, CH_4, collected in conditions of experiment 3 (Figure 4a and Table 1). As the amount of air in the closed vials was fixed and was the same for all samples, and assuming that N_2 will not react with MXenes, the amount of CH_4 divided by the amount of N_2 (from air in the vials) gives the relative amount of CH_4 formed in the reaction. Among two titanium carbide MXenes (Ti_2C and Ti_3C_2), CH_4 was produced much faster from Ti_2C than from Ti_3C_2, indicating that the transformation rate of the three atomic layer thick Ti_2C MXene is higher than the five atomic layer thick Ti_3C_2 MXene. Similar relative reactivities of these MXenes have been reported previously.[21] This comparison gives a direct estimate of the effect of monolayer thickness within the same chemical composition and bonding on the reactivity of the 2D material. In contrast, both Ti_3C_2 and Ti_3CN have a five atomic layer thick monolayer, but compared with Ti_3C_2, Ti_3CN reacts faster, as evidenced by a higher CH_4 evolution rate (Figure 4a). In the structure of this titanium carbonitride MXene, N atoms randomly substitute C atoms in the X element sublattice,[33] thus either one acts as defects in the structure of another, and defected 2D material, as expected, has higher reactivity, perhaps explaining why Ti_3CN reacts faster than Ti_3C_2 MXene. This comparison gives a direct estimate of the effects of composition and defects on chemical properties of 2D materials with the same monolayer thickness. At this point, we should also mention that other factors, such as MXene flake size and the extent of exfoliation, presence of M and X vacancies, distribution of surface functional groups, *etc.* may also contribute to the differences in chemical reactivity. Although detailed analysis of all of these factors is needed in future studies, here, we focused on just first of these factors, the relative differences in flake size and exfoliation extent of MXenes measured using dynamic light scattering (DLS) for MXene solutions and atomic force microscopy (AFM) for dried MXene flakes on silicon (Supporting Information Figures S6 and S7, respectively). The results show that the average thickness of our four MXenes is at a similar level (4−5 nm or ∼3 monolayers), whereas the average lateral flake size of Nb_2C is smaller than that of other MXenes. DLS size measurements give consistently smaller diameter values compared to lateral flake size measured by AFM. This is due to a known limitation of the standard DLS (which represents particles of any shape by spheres) when it is used for plate-like colloidal particles of 2D materials; however, the trends in size between our MXenes extracted from DLS are consistent with the AFM data. With the flake size results in mind, it is ever more interesting that Nb_2C, which is a three atomic layer thick monolayer but, in contrast to Ti_2C, is composed of Nb and C, demonstrates strikingly different degradation kinetics compared to Ti_2C (Figure 4a). In fact, although Nb_2C flakes are the smallest, this material shows the lowest degradation rate among the four studied MXenes, thus indicating that the chemistry of 2D material depends not only on the monolayer thickness but also on its chemical composition and the type of bonding within the monolayer. In this regard, again, MXenes provide an interesting opportunity for systematic studies of these effects in their most disentangled form, which was not possible previously with any other family of 2D materials.

To investigate the role of temperature in MXene transformations, we studied kinetics of these processes at 70, 80, and 90 °C. The kinetic curves for each MXene at different temperatures are shown in the Supporting Information (Figure S8), whereas the curves at the same temperature for different MXenes are shown in Figure S9. The rate constants calculated from the slopes of the lines fitting the initial parts of the kinetic curves were further used to produce the corresponding Arrhenius plots (Figure 4b). The activation energies calculated from the slopes of the Arrhenius plots are 1.62, 5.72, 0.31, and 2.43 kJ/mol for Ti_2C, Ti_3C_2, Ti_3CN, and Nb_2C MXenes, respectively.

CONCLUSIONS

In summary, analysis of gaseous products resulting from chemical transformations of MXenes in aqueous environment was demonstrated as a powerful technique to study chemistry of these materials. In particular, a combination of GC and Raman spectroscopy along with solution pH measurements was used as an efficient way to analyze the products of transformations of four different MXenes, including carbides and a carbonitride. According to experimental data, CH_4 is formed during reactions of carbide MXenes in water, whereas both CH_4 and NH_3 are formed during transformations of the Ti_3CN carbonitride MXene in water.

We further illustrate how to use the fundamental advantages provided by MXenes to disentangle and analyze the effects of monolayer thickness and composition on chemical properties of 2D materials. Transformation rates of MXenes with common transition metal in aqueous environment depend on the monolayer thickness and, additionally, are higher for Ti_3CN carbonitride compared to those of pure carbide MXenes. However, two MXenes with the same monolayer thickness but different transition metals in their structure (for example, Ti_2C and Nb_2C) may have vastly different chemical reactivities, thus demonstrating that chemical properties of 2D materials also depend on their chemical composition and type of bonding within the monolayer when the monolayer thickness and structure are otherwise the same. In this context, the effects of flake size are less significant compared to the effects of monolayer thickness and composition. These results will be important for fundamental studies into chemistry of MXenes and other 2D materials and will also provide guidelines for development of many practical applications of MXenes where their stability is of paramount concern.

METHODS

Synthesis of MAX Powders. Ti_2AlC was synthesized by mixing TiC (typically 2 μm size powder, 99.5%, Alfa Aesar), Ti (−325 mesh, 99.5%, Alfa Aesar), and Al (−325 mesh, 99.5%, Alfa Aesar) powders in a 0.85:1.15:1.05 molar ratio for 12 h, followed by heating at 10 °C/min to 1400 °C and holding at this temperature for 4 h under Ar flow.

https://dx.doi.org/10.1021/acsnano.0c03602
ACS Nano 2020, 14, 10251−10257

Ti_3AlC_2 was synthesized by mixing Ti, Al, and graphite (−325 mesh, 99%, Alfa Aesar) powders in a 3:1.1:1.88 molar ratio for 12 h, followed by heating at 10 °C/min to 1550 °C and holding at this temperature for 2 h under Ar flow. Ti_3AlCN was synthesized by mixing Ti, AlN (10 μm size powder, 98%, Sigma-Aldrich), and graphite powders in a 3:1:1 molar ratio for 12 h, followed by heating at 10 °C/min to 1500 °C and holding at this temperature for 2 h under Ar flow. Nb_2AlC was synthesized by mixing Nb (−325 mesh, 99.8%, Alfa Aesar), Al, and graphite powders in a 2:1.1:1 molar ratio for 12 h, followed by heating at 5 °C/min to 1600 °C and holding at this temperature for 4 h under Ar flow. The resulting samples of MAX phase ceramics were manually crushed by mortar and pestle.

Synthesis of MXenes and Sample Preparation. Synthesis of Ti_2C and Ti_3C_2 MXenes was described previously.[21] The as-synthesized powder of a MAX phase (Ti_2AlC or Ti_3AlC_2, 0.5 g, 325 mesh, particle size <38 μm) was slowly added to the etchant prepared by dissolving 0.5 g of LiF (97%, Alfa Aesar) in 5 mL of 9 M HCl (36 wt %, Alfa Aesar) in a plastic centrifuge tube. The mixture was stirred for 36 h at 35 °C.

Ti_3CN MXene was synthesized from Ti_3AlCN MAX phase.[34] First, 0.5 g of Ti_3AlCN powder (325 mesh, particle size <38 μm) was slowly added to the etchant, prepared by dissolving 0.8 g of LiF in 10 mL of 9 M HCl in a plastic centrifuge tube. The mixture was stirred for 18 h at 40 °C.

Nb_2C MXene was synthesized from Nb_2AlC MAX phase. First, 0.5 g of Nb_2AlC powder (325 mesh, particle size <38 μm) was slowly added to the etchant, prepared by dissolving 1.0 g of LiF in 10 mL of 12 M HCl in a plastic centrifuge tube. The mixture was stirred for 96 h at 60 °C.

After being etched, the mixtures were washed with DI water several times until the pH of the supernatant reached ∼6. MXene aqueous colloidal solutions were obtained *via* 30 min room temperature bath ultrasonication (Bransonic M2800H) followed by 1 h centrifugation (Thermo Fisher Scientific Sorvall ST8 Centrifuge) at 3500 rpm. DI water used in this study was not deaerated. The concentrations of the freshly prepared MXene colloidal solutions were measured by weight after drying five aliquots (500 uL each) of the solution on small pieces of weighing paper and averaging the results. The UV−vis spectra and photographs of as-prepared MXene colloids are shown in Figure S1. Each fresh as-received MXene colloidal solution was used to carry out experiments 1−3 as described below.

For experiment 1 (Figure S2a), four 10 mL headspace vials (Wheaton, 18 mm diameter) were fully filled with MXene colloidal solutions to the rim to ensure that no air bubbles remained in the vial and sealed by a threaded cap with septum. A Metcal 22 gauge polypropylene needle (to avoid potential hydrogen evolution due to reaction of a metal needle with the acidic aqueous liquid) was inserted into each vial through the septum, and the vials were placed upside down into a large beaker partially filled with DI water so that the open ends of the plastic needles were submerged into water for the entire duration of the experiment to prevent air coming into the system while providing an outlet for liquid pushed out of the vials by the evolving gas. The whole setup was placed in a 70 °C oven to accelerate the reaction. The initial concentrations of different MXenes used in this experiment were 3.83, 2.80, 3.74, and 1.10 mg/mL for Ti_2C, Ti_3C_2, Ti_3CN, and Nb_2C, respectively.

For experiment 2 (Figure S2b), 10 mL of each MXene colloidal solution was transferred into a 20 mL glass vial (Wheaton, borosilicate glass vial with polypropylene foamed polyethylene lined screw cap) and kept in a 70 °C sand bath until complete degradation. The pH of the solution was measured every day (for Ti_2C MXene solution it was measured every 2 h) after the sample was cooled to room temperature. The vial was placed back into the sand bath immediately after pH measurement. The measurements were carried out until pH of the solution became stable, indicating complete degradation of the MXene, which was also evident visually. After that, the dispersions were centrifuged at 4500 rpm for 20 min to precipitate the solids. The sediment from degradation of each MXene was collected, rinsed with DI water, and analyzed with Raman spectroscopy. In addition, the supernatant from Ti_3CN degradation was collected and analyzed in liquid form by ATR FTIR. The initial concentrations of different batches of MXenes used in this experiment are shown in Figure S5 (Supporting Information).

For experiment 3 (Figure S2c), 6 mL of each MXene solution was transferred into a 10 mL headspace vial, sealed, and placed upside down to prevent gas escape through the cap. These vials contained around half the volume of ambient air in addition to the MXene colloidal solution. The vials were stored at 70, 80, and 90 °C, correspondingly, in an oven, and Raman spectroscopy was used to analyze the gas phase directly through the walls of the vials over time without opening them upon being cooled to room temperature. After the measurement, the vials were immediately returned back to the oven at the corresponding temperature until the next measurement (typically on the following day except Ti_2C MXene that was measured every 2 h). The initial concentrations of different batches of MXenes used in this experiment are shown in Figures S8 and S9 (Supporting Information).

ASSOCIATED CONTENT

Supporting Information

The Supporting Information is available free of charge at https://pubs.acs.org/doi/10.1021/acsnano.0c03602.

UV−vis spectra and photographs of MXene aqueous colloidal solutions; schematics of experiments 1−3; bond length calculation from rotational Raman spectrum of the gas phase collected during transformation of Ti_2C in water; EDS and SEM of the solid degradation products from MXenes; pH values of MXene aqueous colloidal solutions kept at 70 °C; DLS data for MXene colloidal solutions; AFM images and line scan profiles for MXene flakes on Si wafers; degradation kinetics of MXenes in aqueous solutions at 70, 80, and 90 °C (PDF)

AUTHOR INFORMATION

Corresponding Author

Vadym N. Mochalin − *Department of Chemistry and Department of Materials Science & Engineering, Missouri University of Science & Technology, Rolla, Missouri 65409, United States;* orcid.org/0000-0001-7403-1043; Email: mochalinv@mst.edu

Author

Shuohan Huang − *Department of Chemistry, Missouri University of Science & Technology, Rolla, Missouri 65409, United States*

Complete contact information is available at: https://pubs.acs.org/10.1021/acsnano.0c03602

Notes

The authors declare no competing financial interest.

ACKNOWLEDGMENTS

The authors thank G. Hulliung (Missouri S&T) for help with MXene synthesis and pH measurements. This work was partially supported by the National Science Foundation under Grant No. MoMS 1930881.

REFERENCES

(1) Naguib, M.; Kurtoglu, M.; Presser, V.; Lu, J.; Niu, J.; Heon, M.; Hultman, L.; Gogotsi, Y.; Barsoum, M. W. Two-Dimensional Nanocrystals: Two-Dimensional Nanocrystals Produced by Exfoliation of Ti_3AlC_2. *Adv. Mater.* **2011**, *23*, 4248−4253.

(2) Naguib, M.; Mochalin, V. N.; Barsoum, M. W.; Gogotsi, Y. 25th Anniversary Article: MXenes: A New Family of Two-Dimensional Materials. *Adv. Mater.* **2014**, *26*, 992−1005.
(3) Alhabeb, M.; Maleski, K.; Anasori, B.; Lelyukh, P.; Clark, L.; Sin, S.; Gogotsi, Y. Guidelines for Synthesis and Processing of Two-Dimensional Titanium Carbide ($Ti_3C_2T_x$ MXene). *Chem. Mater.* **2017**, *29*, 7633−7644.
(4) Naguib, M.; Mashtalir, O.; Carle, J.; Presser, V.; Lu, J.; Hultman, L.; Gogotsi, Y.; Barsoum, M. W. Two-Dimensional Transition Metal Carbides. *ACS Nano* **2012**, *6*, 1322−1331.
(5) Dong, Y.; Chertopalov, S.; Maleski, K.; Anasori, B.; Hu, L.; Bhattacharya, S.; Rao, A. M.; Gogotsi, Y.; Mochalin, V. N.; Podila, R. Saturable Absorption in 2D Ti_3C_2 MXene Thin Films for Passive Photonic Diodes. *Adv. Mater.* **2018**, *30*, 1705714.
(6) Yi, J.; Du, L.; Li, J.; Yang, L.; Hu, L.; Huang, S.; Dong, Y.; Miao, L.; Wen, S.; Mochalin, V. N; Zhao, C.; Rao, A. M Unleashing the Potential of Ti_2CT_x MXene as a Pulse Modulator for Mid-Infrared Fiber Lasers. *2D Mater.* **2019**, *6*, 045038.
(7) Chertopalov, S.; Mochalin, V. N. Environment Sensitive Photoresponse of Spontaneously Partially Oxidized $Ti_3C_2T_x$ MXene Thin Films. *ACS Nano* **2018**, *12*, 6109−6116.
(8) Xu, S.; Dall'Agnese, Y.; Wei, G.; Zhang, C.; Gogotsi, Y.; Han, W. Screen-Printable Microscale Hybrid Device Based on MXene and Layered Double Hydroxide Electrodes for Powering Force Sensors. *Nano Energy* **2018**, *50*, 479−488.
(9) Kim, S. J.; Koh, H. J.; Ren, C. E.; Kwon, O.; Maleski, K.; Cho, S. Y.; Anasori, B.; Kim, C. K.; Choi, Y. K.; Kim, J.; Gogotsi, Y.; Jung, H. T. Metallic $Ti_3C_2T_x$ MXene Gas Sensors with Ultrahigh Signal-To-Noise Ratio. *ACS Nano* **2018**, *12*, 986−993.
(10) Li, G.; Kushnir, K.; Dong, Y.; Chertopalov, S.; Rao, A. M.; Mochalin, V. N.; Podila, R.; Titova, L. V. Equilibrium and Non-Equilibrium Free Carrier Dynamics in 2D $Ti_3C_2T_x$ MXenes: THz Spectroscopy Study. *2D Mater.* **2018**, *5*, 035043.
(11) Li, G.; Amer, N.; Hafez, H.; Huang, S.; Turchinovich, D.; Mochalin, V. N.; Hegmann, F. A.; Titova, L. V. Dynamical Control over Terahertz Electromagnetic Interference Shielding with 2D $Ti_3C_2T_y$ MXene by Ultrafast Optical Pulses. *Nano Lett.* **2020**, *20*, 636−643.
(12) Zhang, C. J.; Pinilla, S.; McEvoy, N.; Cullen, C. P.; Anasori, B.; Long, E.; Park, S.-H.; Seral-Ascaso, A.; Shmeliov, A.; Krishnan, D.; Morant, C.; Liu, X.; Duesberg, G. S.; Gogotsi, Y.; Nicolosi, V. Oxidation Stability of Colloidal 2D Titanium Carbides (MXenes). *Chem. Mater.* **2017**, *29*, 4848−4856.
(13) Lipatov, A.; Alhabeb, M.; Lukatskaya, M. R.; Boson, A.; Gogotsi, Y.; Sinitskii, A. Effect of Synthesis on Quality, Electronic Properties and Environmental Stability of Individual Monolayer Ti_3C_2 MXene Flakes. *Adv. Electron. Mater.* **2016**, *2*, 1600255.
(14) Habib, T.; Zhao, X.; Shah, S. A.; Chen, Y.; Sun, W.; An, H.; Lutkenhaus, J. L.; Radovic, M.; Green, M. J. Oxidation Stability of $Ti_3C_2T_x$ MXene Nanosheets in Solvents and Composite Films. *NPJ. 2D Mater. Appl.* **2019**, *3*, 8.
(15) Li, G.; Jiang, K.; Zaman, S.; Xuan, J.; Wang, Z.; Geng, F. Ti_3C_2 Sheets with an Adjustable Surface and Feature Sizes to Regulate the Chemical Stability. *Inorg. Chem.* **2019**, *58*, 9397−9403.
(16) Natu, V.; Hart, J. L.; Sokol, M.; Chiang, H.; Taheri, M. L.; Barsoum, M. W. Edge Capping of 2D-MXene Sheets with Polyanionic Salts to Mitigate Oxidation in Aqueous Colloidal Suspensions. *Angew. Chem., Int. Ed.* **2019**, *58*, 12655−12660.
(17) Zhao, X.; Vashisth, A.; Prehn, E.; Sun, W.; Shah, S. A.; Habib, T.; Chen, Y.; Tan, Z.; Lutkenhaus, J. L.; Radovic, M.; Green, M. J. Antioxidants Unlock Shelf-Stable $Ti_3C_2T_x$ (MXene) Nanosheet Dispersions. *Matter* **2019**, *1*, 513−526.
(18) Mashtalir, O.; Cook, K. M.; Mochalin, V. N.; Crowe, M.; Barsoum, M. W.; Gogotsi, Y. Dye Adsorption and Decomposition on Two-Dimensional Titanium Carbide in Aqueous Media. *J. Mater. Chem. A* **2014**, *2*, 14334−14338.
(19) Naguib, M.; Mashtalir, O.; Lukatskaya, M. R.; Dyatkin, B.; Zhang, C.; Presser, V.; Gogotsi, Y.; Barsoum, M. W. One-Step Synthesis of Nanocrystalline Transition Metal Oxides on Thin Sheets of Disordered Graphitic Carbon by Oxidation of MXenes. *Chem. Commun.* **2014**, *50*, 7420−7423.
(20) Lee, Y.; Kim, S. J.; Kim, Y. J.; Lim, Y.; Chae, Y.; Lee, B. J.; Kim, Y. T.; Han, H.; Gogotsi, Y.; Ahn, C. W. Oxidation-Resistant Titanium Carbide MXene Films. *J. Mater. Chem. A* **2020**, *8*, 573−581.
(21) Huang, S.; Mochalin, V. N. Hydrolysis of 2D Transition-Metal Carbides (MXenes) in Colloidal Solutions. *Inorg. Chem.* **2019**, *58*, 1958−1966.
(22) Philipp, W. H. *Chemical Reactions of Carbides, Nitrides, and Diborides of Titanium and Zirconium and Chemical Bonding in These Compounds*; NASA-TN-D-3533; NASA Lewis Research Center, August 1966; pp 1−20.
(23) Sneed, M. C. The Metalic Borides, Carbides, Silicides, and Related Compounds. *Comprehensive Inorganic Chemistry*; Van Nostrand: New York, 1953; Vol. *7*, pp 251−292.
(24) Remy, H. Fourth Main Group of the Periodic System: Carbon−Silicon Group. *Treatise on Inorganic Chemistry*, 11th ed.; Elsevier: Amsterdam, 1956; Vol. *1*, pp 409−560.
(25) Avgustinik, A. I.; Drozdetskaya, G. V.; Ordan'yan, S. S. Reaction of Titanium Carbide with Water. *Sov. Powder Metall. Met. Ceram.* **1967**, *6*, 470−473.
(26) Wang, C.; Pan, Y. L.; Hill, S. C.; Redding, B. Photophoretic Trapping-Raman Spectroscopy for Single Pollens and Fungal Spores Trapped in Air. *J. Quant. Spectrosc. Radiat. Transfer* **2015**, *153*, 4−12.
(27) Du, Z.; Zhang, X.; Xi, S.; Li, L.; Luan, Z.; Lian, C.; Wang, B.; Yan, J. *In Situ* Raman Spectroscopy Study of Synthetic Gas Hydrate Formed by Cold Seep Flow in The South China Sea. *J. Asian Earth Sci.* **2018**, *168*, 197−206.
(28) Su, T.; Peng, R.; Hood, Z. D.; Naguib, M.; Ivanov, I. N.; Keum, J. K.; Qin, Z.; Guo, Z.; Wu, Z. One-Step Synthesis of Nb_2O_5/C/Nb_2C (MXene) Composites and Their Use as Photocatalysts for Hydrogen Evolution. *ChemSusChem* **2018**, *11*, 688−699.
(29) Seredych, M.; Shuck, C. E.; Pinto, D.; Alhabeb, M.; Precetti, E.; Deysher, G.; Anasori, B.; Kurra, N.; Gogotsi, Y. High-Temperature Behavior and Surface Chemistry of Carbide MXenes Studied by Thermal Analysis. *Chem. Mater.* **2019**, *31*, 3324−3332.
(30) Sun, C.; Xu, D.; Xue, D. Direct *In Situ* ATR-IR Spectroscopy of Structural Dynamics of $NH_4H_2PO_4$ in Aqueous Solution. *CrystEngComm* **2013**, *15*, 7783−7791.
(31) Thämer, M.; De Marco, L.; Ramasesha, K.; Mandal, A.; Tokmakoff, A. Ultrafast 2D IR Spectroscopy of the Excess Proton in Liquid Water. *Science* **2015**, *350*, 78−82.
(32) Li, Y.; Huang, S.; Wei, C.; Wu, C.; Mochalin, V. N. Adhesion of Two-Dimensional Titanium Carbides (MXenes) and Graphene to Silicon. *Nat. Commun.* **2019**, *10*, 3014.
(33) Du, F.; Tang, H.; Pan, L.; Zhang, T.; Lu, H.; Xiong, J.; Yang, J.; Zhang, C. J. Environmental Friendly Scalable Production of Colloidal 2D Titanium Carbonitride MXene with Minimized Nanosheets Restacking for Excellent Cycle Life Lithium-Ion Batteries. *Electrochim. Acta* **2017**, *235*, 690−699.
(34) Hart, J. L.; Hantanasirisakul, K.; Lang, A. C.; Anasori, B.; Pinto, D.; Pivak, Y.; van Omme, J. T.; May, S. J.; Gogotsi, Y.; Taheri, M. L. Control of MXenes' Electronic Properties through Termination and Intercalation. *Nat. Commun.* **2019**, *10*, 522.

https://dx.doi.org/10.1021/acsnano.0c03602
ACS Nano 2020, 14, 10251−10257